DOE/ER/12022--2

DE84 005193

PROGRESS REPORT

ON

HEAT TRANSFER IN OSCILLATORY FLOW

by

D. P. Telionis and T. E. Diller

DOE Contract DE-AS05-82ER12022

REPORTING PERIOD: JAN. 83 - DEC. 83

TABLE OF CONTENTS

1. PROGRESS & ACCOMPLISHMENTS

1.A. WATER TUNNEL WORK

We have proposed for this project significant changes to our facility and our experimental arrangement. Some of the changes accomplished were also necessary for work being conducted with the support of the AFOSR. It turned out that we were also given the opportunity during this reporting period to upgrade the entire system of our Laser-Doppler Velocimetry and Data Acquisition. A considerable amount of time was therefore devoted to

(a) changing our LDV arrangement from a forward-scatter to a backward-scatter mode,

(b) operating with counters instead of trackers,

(c) traversing with mirrors instead of optical benchs,

(d) feeding signals digitally to the computer, thus eliminating Digital-to-Analog (D/A) and Analog-to-Digital (A/D) converters.

We describe here briefly some of the work which was necessary for upgrading the water tunnel experimental rig, as well as some of our results on the unsteady flow on circular cylinders. A detailed account of the calibration of the water tunnel is included in a report (see publication No. 2.A.4) a first draft of which is being submitted with this package. We are presently conducting careful experiments on pulsating flows over cylinders and we will be reporting the results shortly.

1.A.1 Facility Modifications and Additions

In this section we describe the necessary modifications on the facilities and provide examples of the calibration data. It should be emphasized that for the past 6 years, our experimental work on unsteady flows was performed with a steady stream. Unsteadiness was introduced by dynamic motion of the model or part of it. Modifications were proposed and carried out to convert the tunnel to an oscillating tunnel. This, of course, required extra efforts to reduce the turbulence in the tunnel and recalibrate the facility.

a. Rotating Vane

To control the mean flow, a rotating vane was installed immediately above the test section as shown in Fig. 1. This vane was coupled to a HELLER DC motor with variable speed control. The unit controls automatically the speed to within ± 0.5% of the set value. It is also equipped with an optical encoder which can be interphased directly with the laboratory computer.

b. By-Pass System

A very significant factor in studies of unsteady aerodynamics is the amplitude of oscillation. To our knowledge, in all facilities employing some mechanical method for control of the frequency of oscillation, the amplitude ends up being a function of the frequency. A separate system is necessary, if one desires to control independently both the amplitude and the frequency of the oscillation. In our case this was accomplished by a by-pass pipe and a by-pass valve as shown in Fig. 1. The position of this valve controls the efficiency of the rotating vane. Charts of the performance of these controls have been constructed and are included in an engineering report (see 2.A.4).

c. Quality Control

Any periodicity externally added to a tunnel generates free-stream turbulence. Existing unsteady flow facilities operate with turbulence levels of the order of 1%. Careful studies require much lower turbulence levels. To quiet the flow in our tunnel we studied the literature on honeycombs and screens (Dryden and Abbott, 1948; Schubauer, Spangenberg and Klebanoff, 1948; Loehrke and Nagib, 1976; Wigeland, et al, 1978; Tan-atichat, et al, 1982) and contacted personally an expert in the field (Nagib, 1983). As a result of our investigations, we installed in the settling chamber a second set of finer honeycombs and 3 sets of fine screens.

Typical results are shown in Tables 1 and 2, obtained with an LDV tracker and counter respectively. In this table, the tunnel speed and the by-pass valve are controlled independently. It is surprising that the by-pass system influences greatly the turbulence level, even though it is far upstream of the test section. We have also performed an exhaustive study of turbulence frequency spectra examples of which are shown in Fig. 2.

d. Pressure Control

The acceleration and deceleration of large masses of water induce fluctuations of pressure that may exceed the strength of the plexiglass structure. Moreover, the efficient operation of hydrogen bubbles require pressure levels lower than the atmosphere. To control the pressure level in the tunnel, we have installed a water trap and piping which connects the system to a vacuum pump. A separate level indicator was added and numerous valves as shown in Fig. 3.

1.A.2 Instrumentation and Data Acquisition

a. Backward Scatter Mode

Accurate traversing of the measuring volume can be accomplished with LDV in the backward-scatter mode. Moreover, our plans to measure vorticity by shifting the beams can be implemented much easier in the backward scatter mode. A one-channel TSI system was purchased in the Spring of 1982 and was tested in the forward-scatter mode. Bragg cells were also included and their operation was compared to the performance of our DISA units.

b. Traversing of Measuring Volume

A special system was designed and constructed for traversing the measuring volume via mirrors. Such a system should meet some basic requirements: (i) it should allow very accurately controlled displacements, (ii) it should permit the displacement of the measuring volume in two directions, parallel and perpendicular to the flow, (iii) it should be controlled directly by the laboratory computer, (iv) it should be free of vibrations and finally, (v) it should allow the rotation of the beams about their bisector so that components of the velocity in any direction can be measured.

The system we designed and constructed is shown schematically in Fig. 4. The train of TSI optics is mounted on a linear translator which allows the entire system to move in the x-direction. The parallel beams are then reflected twice from mirrors as shown in the figure and pass through a lens to converge at the measuring volume. The upper mirror together with the lens translates in the vertical direction to facilitate motion of the measuring volume along the y-axis. Details of the mirror tower are shown in Fig. 5. Both motions are controlled by stepping motors interphased with the laboratory computer. In this way steps as small as 1/100 mm can be implemented easily. Moreover, successive steps Δx and then Δy may displace the measuring volume along any inclined straight line.

c. Signal Processing

The LDV signals we process now with TSI counters. We have recently purchased a second counter and we now have the capability to measure the instantaneous value of vorticity, the cross-correlation of velocity, or two velocity components.

We found that counters are far superior to trackers for the type of work we are interested in. The main two reasons are the following: (i) For large fluctuations of the flow, a tracker may loose the signal in the middle of an averaging operation which will require repeating all of the measurements. A counter instead operates with the same efficiency at any level of its measuring scale. (ii) Automatic traversing across the boundary layer brings a tracker in regions of its scale which do not allow accurate measurement. This requires the constant attention of the operator who has to switch the tracker to a lower range at least once in a boundary layer profile. This is not necessary with a counter and an entire velocity profile can be obtained automatically.

Our two counters are equipped with a master and a slave interface respectively to allow them to talk directly to our laboratory computer. This is another serious advantage of the present system. The signals from the photomultipliers are processed digitally and the information is fed directly to the computer without the interference of digital to analog and analog to digital converters.

d. Data Acquisition

A major improvement in our experimental facilities has been the acquisition of a MINC-11 computer with all the necessary boards (D/A and A/D converters, digital or analog output, multiplexer, etc.). We have already prepared and tested software for all the necessary operations in our laboratory. Many of these tasks were performed before by an HP5420 which of course is still available. However now we have the flexibility to control and define the way of manipulating our data on line. Moreover, we can dump our raw data directly to an IBM 370 for further processing.

The laboratory computer is the heart of the entire system. It controls all other instruments, it displaces the measuring volume, it checks continuously for the quality of the signal, it receives the data, it manipulates them on the line and it stores them. The particular arrangement for the present project is shown schematically in Fig. 6. An outline of the flow chart of this operation is shown in Fig. 7. The computer performs conditional averaging of the periodic signal at a point and then orders the stepping motors to proceed to the next position. According to the specific application, the LDV counters are interrogated by the computer to insure proper operation of the system. The software provides for input from encoders which would insure that the micropositioning commands have been executed properly. Moreover, the general condition of the tunnel will be recorded, namely speed, temperature of the medium, and frequency of the imposed oscillation.

Most recently, one of our proposals to DOD for equipment was funded. We are now in the process of putting together a very powerful system for acquisition and processing of data. This system provides two ultra-high speed, 16-channel, data sampling capabilities. In addition, real-time data-processing capabilities are provided by two minicomputers (MASSCOMP 560) with output via floppy disk, printer, CRT display, and digital plotting. Large-scale computing is provided by the main frame (Data General MV 8000) connected directly to the mini. The mini controls the experiment and the data acquisition. This system, built around a real-time UNIX operating system is the state-of-the-art in data acquisition. Our work on the MINC 11, interfacing instruments with the computer and preparing software for our particular applications has paved the way for the more powerful machines that we will soon have. We will therefore be able to get full advantage of their speed and versatility, almost immediately after they become available.

1.A.3 Experimental Results

Exhaustive measurements were obtained to document the efficiency of the by-pass system in controling the amplitude of the oscillation. Moreover, the quality of the flow in the tunnel has also been investigated carefully for complete matrix of the parameters. These data are included in the engineering report on the water tunnel which is being submitted together with this report.

Velocity measurements were also obtained around a circular cylinder with emphasis at the neighborhood of separation.

1B. WIND TUNNEL WORK

The three areas of work using wind tunnels (construction of facilities, synthesis of instrumentation and experiments) have progressed well. The construction of all of the necessary facilities is nearly complete. The basic instrumentation has been tested and calibrated and additional instrumentation is being developed as the need arises. A good set of experimental data was obtained and will be presented at a national engineering conference in February, 1984. Additional papers are currently being reviewed. Details of each of these three project areas are given in the follwing sections.

1B.1 Facilities

Three separate wind tunnel/heat transfer facilities have been built and used for this project. The small wind tunnel (test section 25cmx 36cm) was designed, built and calibrated during the first year of the project. Subsequently, it has been used to obtain the initial heat transfer and pressure distribution data in unsteady flow. The large wind tunnel (test section 53cmx75cm) has been built and calibrated in steady flow. The third facility is a small wind tunnel designed for calibration of the local heat flux gages. Details of these facilities follow.

a. Small Wind Tunnel

A few minor modifications were made to the small wind tunnel (Fig. 8) to increase the attainable pulsation frequency and amplitude. The unifromity of this tunnel is within ± 1.5% and the turbulence intensity in steady flow is 0.2%. The velocity waveforms obtained were well defined and very nearly sinusoidal. Details of the unsteady performance are given in the accompanying report [2A2] and Paper [2A6]. This wind tunnel was used to obtain initial heat transfer and pressure distribution results for a cylinder in steady and pulsatile crossflow.

b. <u>Large Wind Tunnel</u>

The large wind tunnel is of the same design as the small tunnel, but over twice as large. The small tunnel was originally built to test the design and feasibility for producing a good pulsating flow. Moreover, because of the much longer lead-time to build the large tunnel, initial heat transfer results were obtained much faster with the small tunnel. The large tunnel is similar to the facility originally described in the proposal. It will provide the ability to achieve larger Reynolds number, higher pulsation amplitudes and better experimental resolution and control. Initial calibration in steady flow indicates ± 1.0% uniformity of the mean flow and a free stream turbulence intensity of 0.2%. It should be operating in the unsteady mode by the end of 1983.

c. <u>Calibration Facility for Local Heat Flux Gages</u>

A facility was designed and built for calibrating the local heat flux gages in convective flows similar to those used in the test cylinder (Fig. 9). There are two reasons why this is an important part of the project. First, to insure accurate data calibration of the gage independent of the manufacturer's calibration is advisable. Second, all other calibrations of these gages are done by radiation. Previously the results have simply been assumed to be also accurate for convection.

The calibration facility consists of a small wind tunnel (10cmx10cm exit) which is driven by a small high-pressure blower. The flow (steady) impinges on a guarded hot plate containing the heat flux gage. The hot plate is designed to allow accurate measurements of the surface heat flux which can then be correlated with the gage output.

The test results were compared with a previous nonlinear theory (Striegl and Diller, 1984) for the performance of these gages in convection. This contrasts with the output from the standard radiation calibration, which is linear. The test results correlated with the nonlinear theory to within 1.5% (95% confidence internal). This is well within the estimated accuracy of the system of 2.5%. Details of the apparatus and test results are in a paper [2B1] that has been submitted for presentation at the National Heat Transfer Conference in 1984. Conversations with other researchers who measure local heat transfer (e.g. at NASA, NBS and Pratt and Whitney) rates has revealed much interest in such a convecting calibration system. Apparently no such facility has been developed previously.

1.B.2 Instrumentation

a) Heat Flux Gages

The current heat flux gages are used for time-averaged, local measurements around the cylinder. Although the gage time-response is approximately 300 msec, this is not fast enough for good response at the pulsation frequencies used in the wind tunnel (3.5 Hz to 39.5 Hz). The gages (1/8" diameter) are mounted through a hole in the aluminum test cylinder and positioned flush with the surface. The cylinder is instrumented with thermocouples and heated electrically from the inside. The accuracy of the present gages is estimated at ± 3% to ± 5% depending on the local value of the heat transfer coefficient around the test cylinder. This is very good for measurements of local heat flux. It is planned, however, to obtain additional gages that will allow measurements with slightly better accuracy.

b. Pressure Measurements

The pressure distribution about the circular cylinder was measured by manometers and microphones. Stateic pressure taps where connected in the traditional way to prezoneter tubes to provide the mean pressure distribution. Pressure fluctuations were obtained via B&K microphones. One special model was constructed for the measurements of pressure and is shown in Fig. 10. More details are included in our publication 2.A.6.

c) Automated Data Acquisition System

An automated data acquisition system has been designed and should be operating by the end of 1983. It uses a computer to both position the cylinder and record all of the heat transfer data. This allows large amounts of local data to be obtained, stored, and transferred to the main University computing system for subsequent manipulation and analysis.

The mechanical engineering department has recently acquired a TSI IFA 100 2-channel hot-wire anemometer. This is a new unit which has been designed to be interfaced with a computer for control and data acquisition. This will fit well with the overall data system being developed.

d) Fast-Response Heat Flux Gages

Because of the importance of time-varying heat flux in pulsating flow, we have undertaken development of a fast-response heat flux gage. The goal is to obtain a gage with good resonse characteristics in the range of 1 Hz to 100 Hz. Very few measurements have been obtained in this range. Thin-film sensors have previously been used to measure the frequency content of the heat transfer, but calibration to obtain the magnitude of the heat flux has not been done (e.g., Boulos and Pei, 1974). With the calibration facility which has already been developed (see Section 1B.1.c), absolute magnitudes of the heat flux should be readily achievable. This was not in the original project description, but has been added to further basic understanding of the unsteady phenomena.

1.B.3 Experimental Results

Initial heat transfer and surface pressure measurements were taken on a 6.0cm diameter cylinder in the small wind tunnel. Tests were performed for steady flow and pulsation frequencies from 3.5 to 39.5 Hz. This range corresponds to frequencies below, at, and above the natural shedding frquency of the cylinder crossflow. The time-averaged heat transfer, mean surface pressure, and fluctuating surface pressure were detailed around the cylinder. The heat transfer was increased by the pulsation at all positions around the cylinder with the largest percentage increases near the separation point. The mean surface pressure distribution was not greatly affected by the pulsation. The fluctuating component of the pressure, however, was significantly increased by the pulsation and was strongly dependent on the frequency. Further details are given in the paper [2A6] and thesis [2A5] enclosed.

1.C. NUMERICAL AND ANALYTICAL WORK

A computer code was developed for the calculation of steady and unsteady heat transfer over the attached portion of the boundary layer. The equations of momentum and energy were recast in their finite-difference form.

To the knowledge of the investigators, a complete finite-difference scheme has not been employed yet in the calculation of the steady heat transfer problem. Considering the fact that we are using grids of the order of 100x100 points, our solution is for all practical purposes an exact solution. Errors should be confined to the 6th decimal point.

Extension of the method to unsteady flow encounters a serious difficulty. The shedding of vortices over a circular cylinder, natural or forced, induces a disturbance in the upstream potential flow. As a result, the point of stagnation is oscillating. Thus, in the immediate neighborhood of the stagnation point the outer flow velocity as well as the velocity near the wall periodically change direction. It is therefore impossible to define an initial condition in order to march the calculation in the axial direction.

This difficulty was surpassed by matching a solution of the full Navier Stokes equation for the problem of oscillating stagnation on a flat instead of a curved wall. This is essentially an inner expansion, valid for small values of the distance from the origin and small ratios of boundary layer thickness to the radius of the cylinder.

For a flow stagnating on a wall as in the figure, the full Navier Stokes equations read

$$u_x + v_y = 0 \tag{1}$$

$$u_t + uu_x + vu_y + \frac{1}{\rho} p_x = \nu(u_{xx} + v_{yy}) \tag{2}$$

$$v_t + uv_x + vv_y + \frac{1}{\rho} p_y = \nu(v_{xx} + v_{yy}) \tag{3}$$

$$T_t + uT_x + vT_y = \frac{k}{\rho C} (T_{xx} + T_{yy}) \tag{4}$$

where u,v are the x,y components of the velocity, u=v=0, T=0 at y=0, T,ρ,p are temperature, density and pressure respectively, ν, k and C are the kinematic viscosity, conductivity and specific heat respectively. The outer edge boundary condition incorporates a fluctuation

$$u = ax + 6\cos\omega t + O(1) \tag{5}$$

$$v = -ay + O(y) \tag{6}$$

$$\frac{1}{\rho} p = b[\omega b\sin\omega t - a\cos\omega t] - \frac{a^2}{2} (y^2 + x^2) + H(t) + O(1) \tag{7}$$

$$T = T_\infty \tag{8}$$

as $y^2 + x^2 \to \infty$

A solution can be found in the following form,

$$v = -f(y) \tag{9}$$

$$u = xf'(y) + g(y)\cos\omega t + h(y)\sin\omega t \tag{10}$$

$$\frac{p}{\rho} = m(t) - \nu f' - \frac{f^2}{2} - \frac{x^2a^2}{2} + xb(\omega\sin\omega t - a\cos\omega t) \tag{11}$$

$$T = T(y) \tag{12}$$

provided the functions f,g, h and T satisfy the following ordinary differential equations and boundary conditions

$$\nu f''' + ff'' - f'^2 + a^2 = 0 \qquad (13)$$

$$f'(\infty) \to a,\ f(0) = f'(0) = 0 \qquad (14)$$

$$\nu g'' + fg' - fg' - \omega h + ab = 0 \qquad (15)$$

$$\nu h'' + fh' - f'h + \omega g - \omega b = 0 \qquad (16)$$

$$g(\infty) \to b,\ h(\infty) \to 0,\ g(0) = h(0) = 0 \qquad (17)$$

$$T'' + f\,\frac{\rho C}{k}\,T' = 0 \qquad (18)$$

$$T(0) = T_0,\ T(\infty) \to T_\infty \qquad (19)$$

This system of equations has been solved numerically by modifying a shooting method to handle nonlinear coupled equations. Typical results showing the dimensionless counterparts of the functions f,g and h are displayed in Fig. 11.

This solution has been incorporated in the computer code to provide the initial profiles for the unsteady calculation. The method has then been used to generate the instantaneous velocity and temperature field over the attached region of the boundary layer.

The outer flow solution was assumed to have a Hiemenz mean distribution give by the formula

$$U_e(x) = 3.631(x/D) - 3.275(x/D)^3 - 0.168(x/D)^5 \qquad (20)$$

The unsteady counterpart was given in the form

$$U_e(x,t) = 3.631(x/D) + \beta\cos\omega t \qquad (21)$$

which approximates closely the experimental data. The code is thus readily available to calculate the flow over the attached region of a cylinder in a bundle of other cylinders.

Typical results of the averaged heat transfer are shown in Fig. 12. At the present, we have some difficulties with large amplitudes of oscillation. We do not have yet a solution for ampliutudes corresponding to the natural shedding process. Moreover, the heat transfer in the stagnation region is overpredicted.

2. PUBLICATIONS

2A. Published Documents

The publications that have already been submitted to the DOE are marked by an asterisk. The publications that are being shipped are marked by 2 asterisks.

2.A.1* "Design of Evaluation of a Pulsating Flow Wind Tunnel"
VPI & SU, M.S. Thesis by Amir Tavakoli, October 1982

(Abstract)

A wind tunnel was designed and built to produce a pulsating flow. The pulsation was achieved by a series of shutters (rotating with constant angular velocity) placed upstream of the settling chamber inlet. The system was optimized to obtain nearly sinusoidal velocity waveforms with the highest obtainable amplitudes over the frequency range of 3.4 to 31.3 Hz. The velocity and pressure waveforms are given for different shutters settings and conditions.

It was found that the velocity waveform shape and amplitude, obtained in the test section, are a strong function of pressure build-up in the diffuser upstream of the shutters box. An explanation is given, for various shutters settings and conditions, of how pressure release is achieved and how the pressure waveforms are generated.

2.A.2.* "Pulsating Flow & Heat Transfer Over a Circular Cylinder", Presented at the Symposium on Nonlinear Problems in Energy Engineering, Argonne National Laborotory by B. K. Kim, G. J. Borell, T. E. Diller, M. S. Cramer and D. P. Telionis, April 1983

(Abstract)

Methods of calculation and measurement of heat transfer in periodic flows are discussed. A finite-difference scheme for attached boundary layers is presented. Stagnation flow heat transfer measurements are reported and the technique for extending these measurements to cylindrical models are presented.

2.A.3** "Design and Evaluation of a Pulsating-Flow Wind Tunnel" VPI & SU, Engineering Report No. VPI-E-83-41, by A. Tavakoli, B. K. Kim, G. J. Borell, T. E. Diller and D. P. Telionis, May 1983

(Abstract)

A wind tunnel was designed and built to produce pulsating flow. The pulsation was achieved by a series of shutters placed upstream of the settling chamber inlet. The shutters were rotated with the same angular velocity, but a variety of phase differences were used to affect the velocity wave form in the test section. The system was optimized to obtain nearly sinusoidal velocity waveforms with the highest obtainable amplitudes over the frequency range of 3.4 to 39.5 Hz. Velocity and pressure waveforms are given for different shutters settings and conditions.

It was found that the velocity waveform shape and amplitude, obtained in the test section, are a function of the unsteady pressure variation in the diffuser upstream of the shutters box. An explanation is given, for various shutters settings and conditions, of how pressure release is achieved and how the pressure and velocity waveforms are generated.

2.A.4** "Calibration of the ESM Water Tunnel", Engineering Report, VPI & SU, 1983, by D. P. Telionis, D. Mathioulakis, B. K. Kim and G. S. Jones

(Abstract)

The VPI water tunnel has been recently modified to allow large amplitude mean flow oscillations. This was accomplished by a by-pass system and a rotating vane. Moreover, special attention has been devoted to methods of reducing the turbulence level and improving in general the quality of the flow. In this report we provide a large number of calibration data as well as information on the performance of the disturbing mechanism and the waveforms of the generated flow oscillations.

2.A.5** "Heat Transfer from a Circular Cylinder in a Pulsating Crossflow", VPI & SU, M.S. Thesis by George J. Borell, October 1983

(Abstract)

The effects of organized well-defined harmonic disturbances in the mean crossflow on heat transfer from a circular cylinder were experimentally determined. Local, time-averaged heat transfer data at constant wall temperature is reported for Reynolds numbers between 3×10^4 and 9×10^4. Pulsation amplitudes were generally small (<10 per cent) with frequencies up to and beyond the frequency of natural shedding. Small increases in heat transfer all around the

cylinder are found in pulsating flow. More significant increases occur near the separation point.

A convection calibration for the circular foil heat flux gage used in the heat transfer experiments is included. The convection calibration shows a nonlinear gage response for a 'hot' gage in a convection environment. This is in contrast to the linear calibration curve produced by the standard 'cold' gage radiation technique.

2.A.6** "Pressure and Heat Transfer Measurements Around a Cylinder in Pulsating Crossflow" to be presented at the ASME Fluids Engineering Conference, New Orleans, Feb. 1984, by G. J. Borell, B. K. Kim, W. Ekhaml, T. E. Diller and D. P. Telionis

(Abstract)

The effects of well-defined harmonic disturbances of the mean crossflow past a cylinder were experimentally determined. Pulsation frequencies above and below the natural shedding frequency were used. For most of the frequencies tested, the amplitudes were small (<5%). The time-averaged local heat transfer was measured for a constant temperature surface boundary condition. Measurements of both the mean and fluctuating components of the surface static pressure were measured in the same wind tunnel at the same conditions.

Increases in the heat transfer due to the pulsation were found at all positions around the cylinder. The largest increases were near the separation point. Corresponding changes in the mean static pressure were not observed, although the fluctuating component of the pressure showed significant changes in pulsating flow, particularly near the separation point.

2.B Reports & Papers Under Preparation

2.B.1 "A Convection Calibration Method for Local Heat Flux Gages" by G. J. Borell and T. E. Diller, extended abstract submitted for presentation at the 22nd National Heat Transfer Conference, Niagara Falls, Aug. 1984

(Abstract)

An apparatus for calibrating local heat flux gages in convective air flows is described. Heat transfer was measured using a guarded hot-plate technique from a "hot" gage to a "cold" fluid. The system was used to calibrate Gardon-type circular foil heat flux gages of 1/8" and 1/16" outer diameters. The results indicate a non-linear calibration curve which differs from the linear calibration obtained using the standard radiation technique. The difference matches a previous analysis which accounts for the effect of the temperature distribution in the gage foil. This distribution can be neglected in the standard radiation calibration but is often significant in convection applications.

2.B.2 "Pressure Variations About a Circular Cylinder in Pulsating Cross Flow" by William Ekhaml, ESM Senior Project Report, expected Dec. 1983

(Abstract)

A model of a circular cylinder was designed and constructed. Static pressure taps were machined and appropriate fittings were provided for the installation of 3 B&K microphones. The cylinder was tested in an unsteady tunnel for steady flow as well as pulsating flow with a range of amplitude and frequency of 5-9% and 10-40 Hz respectively. Averaged pressure distributions were obtained for all cases. Instantaneous pressure values were recorded and the results were processed by an FFT in the frequency domain. It appears that for these low amplitudes, the wake does not lock to the free stream disturbance, except perhaps in the immediate neighborhood of the Strouhal frequency.

2.B.3 "Unsteady Head Convection Over a Circular Cylinder", by M. S. Cramer, B. V. Kim and D. P. Telionis, extended abstract submitted for presentation at the 22nd National Heat Transfer Conference, Niagara Falls, Aug. 1984.

(Abstract)

The mass, momentum and energy equations are recast in their finite-difference boundary-layer form. Solutions are obtained for pulsating flows over a circular cylinder. An inner exact solution of the Navier Stokes equation valid in the immediate neighborhood of the stagnation point is obtained separately, to generate the initial condition for the velocity and temperature field. Steady as well as periodic flows are considered. The instantaneous velocity and temperature fields are obtained. It is demonstrated that the average of an unsteady flow problem generates higher heat transfer rates than the corresponding steady flow.

3. PERSONNEL

3.A Engineering Science & Mechanics

Mr. Cramer, Mr. Kim and Mr. Telionis have participated in the second year of work on this project. They have worked on the analytical model whereas the last two have been involved in the expermental effort as well. In the water tunnel work Mr. Costis has been providing some assistance on a part-time basis in the development of data acquisition software. Moreover, Mr. Ekhaml has participated in the calibration of B&K microphones and the collection of unsteady pressure data in the wind tunnel.

Mr. Ekhaml has completed a senior project and is expected to graduate in December 1983. Mr. Kim is working on his Ph.D. dissertation and expects to complete all the requirements in 1984.

3.B. Mechanical Engineering

Mr. Borell, Mr. Andraka, Mr. Campbell and Mr. Diller have participated in the second year of research.

Mr. Borell graduated in September, 1983, with a Master's Degree and is currently working for the Harris Corporation. He was responsible for the heat transfer measurements and development of the heat flux calibration system.

Mr. Andraka has worked part-time on the project for most of the year. In September he became a graduate student and started an NSF fellowship. His immediate responsibility is the completion and calibration of the large wind tunnel and construction of the new data acquisition system.

Mr. Campbell also started graduate school in September, coming from a job with Martin Marietta Aerospace. He is responsible for developing the thin-film gages for measuring time-dependent heat flux.

Both Mr. Andraka and Mr. Campbell should finish their master's degrees in 1984.

REFERENCES

Boulos, M. I., and Pei, D. C. T., "Dynamics of Heat Transfer from Cylinders in a Turbulent Air Stream", Intl. J. Heat Mass Transfer, Vol. 17, 1974, pp. 767-783.

Dryden, H. L. and Abbott, I. H., 1948, "The Design of Low-Turbulence Wind Tunnels", NACA TN 1755.

Loehrke, R. I. and Nagib, H. M., "Control of Free-Stream Turbulence by Means of Honeycombs: A Balance Between Suppression and Generation", Journal of Fluids Engieering, Vol. 98, 343-353, 1976.

Nagib, H. M., private communication, 1983.

Schubauer, G. B., Spangenberg, W. G. and Klebanoff, P. S., 1948, "Aerodynamic Characteristics of Damping Screens", NACA TN 2001.

Striegl, S. A. and Diller, T. E., "The Effect of Entrainment Temperature on Jet Impingement Heat Transfer", accepted for publication in Journal of Heat Transfer, Transactions of the ASME.

Tan-atichat, J., Nagib, H. M. and Loehrke, R. I., "Interaction of Free-Stream Turbulence, with Screens and Grids: A Balance Between Turbulence Scales", Journal of Fluid Mechanics, Vol. 114, pp. 501-528, 1982.

Wigeland, R. A., Ahmed, M. and Nagib, H. M., "Management of Swirling Flows with Application to Wind Tunnel Design", AIAA Journal, Vol. 16, pp. 1125-1131, 1978.

<u>Table 1</u>

Speed of Pump	By Pass Closed fo (kHz)	RMS (mV)	TU (%)	By Pass at Z fo (kHz)	RMS (mV)	TU %	By Pass at 4 fo (kHz)	RMS (mV)	TU (%)	By Pass Open fo (kHz)	RMS (mV)	TU (%)
0.5	107	12	0.16[a]	94	25	0.39	64	351	0.82	55	30	0.81
0.5*	115	6	0.07	104	12	0.17	70	40	0.85	60	35	0.87
1	145	17	0.62	122	17	0.69	83	80	1.44	72	48	1
2	220	30	0.68	180	25	0.69	130	25	0.96	115	20	0.26[c]
3	290	40	0.68	255	38	0.76	180	35	1.028	160		
4	350	8[d]	0.11[e]	290	35	0.6	212	50	1.17	195	55	1.41
4*	360	7	0.09	310	20	0.32	230	50	1.08	210	60	1.42
5	420	15	0.53	360	7	0.09	260	50	0.96	225	60	1.33
5*	410	2[g]	0.015[f]	350	9	0.12	250	60	1.2	230	60	1.30

<u>Table 1</u>: The effect of the bypass system and the tunnel speed on the turbulence level. The speed of the tunnel is represented by the speed of the driving pump in control system values which correspond here roughly to speeds of up to 3m/sec. In the vertical columns f_D is the mean Doppler frequency, RMS is the root mean square of the signal and TU is the turbulence level. The by-pass opening is also marked in values of the control system. The starred rows correspond to tests with no extra honeycomb at the entrance of the test specimen. This instrument displays large discrepancies if the reading is not within a narrow band of the scale. The readings marked by a letter were repeated with a different scale and resulted in the following values of the turbulence level: (a) TU = 0.56%, (b) RMS = 25 mV, (c) TU = 10.8%, (d) RMS = 12 mV, (e) TU = 0.5%, (f) RMS = 15 mV, (g) TU = 0.53%.

Table 2

Speed of Pump	fo (kHz)	RMS (mV)	TU %	fo (kHz)	RMS (mV)	TU %	fo (kHz)	RMS (mV)	TU %	fo (kHz)	RMS (mV)	TU %
	By Pass Closed			By Pass at Z			By Pass at 4			By Pass Open		
0.5	(n=9) (v=2.94) 90	14	0.47	(n=9) (v=2.362) 72	12	0.50	(n=9) (v=1.611) 49	15	0.93	(n=9) (v=1.442) 44	15	1.04
1	(n=8) (v=2.219) 135	14	0.63	(n=80 (v=1.85) 112	14	0.75	(n=8) (v=1.244) 76	15	1.2	(n=8) (v=1.104) 67	15	1.35
2	(n=8) (v=3.342) 203	26	0.77	(n=8) (v=2.709) 165	20	0.74	(n=8) (v=1.887) 115	25	1.32	(n=8) (v=1.734) 109	19	1.09
3	(n=8) (v=4.41) 260	26	0.56	(n=8) (v=3.79) 231	28	0.73	(n=8) (v=2.67) 163	30	1.12	(n=8) (v=2.35) 144	35	1.48
4	(n=8) (v=5.53) 337	30	0.54	(n=8) (v=4.62) 282	30	0.65	(n=8) (v=3.26) 199	40	1.22	(n=8) (v=2.99) 182	50	1.67
5	(n=8) (v=6.63) 404	36	0.54	(n=8) (v=5.63) 343	36	0.64	(n=8) (v=4.04) 246	50	1.23	(n=8) (v=3.65) 223	55	1.5

Table 2: Data similar to Table 1 obtained with a TSI counter.

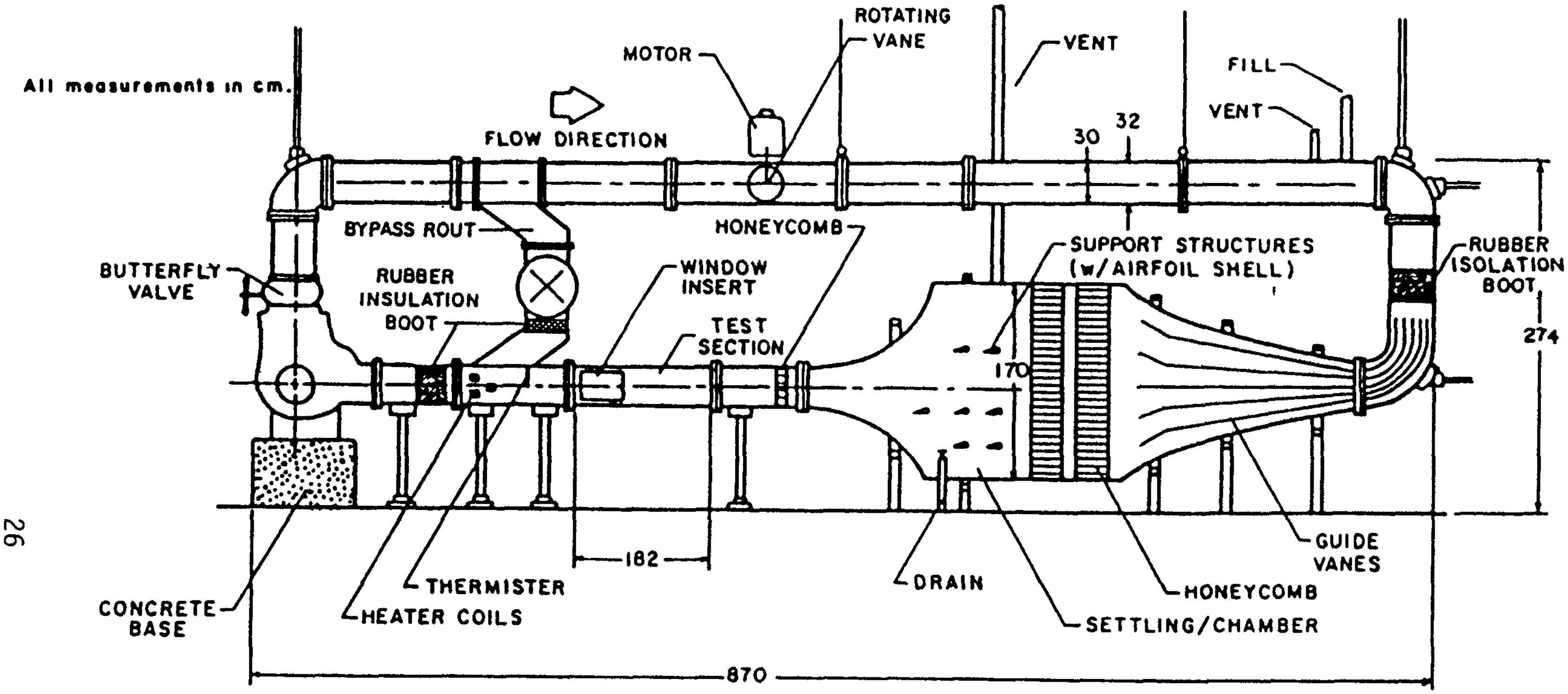

Fig. 1 The ESM water tunnel showing the necessary modifications: A by-pass system and a control valve to short-circuit the pump and a rotating vane with a variable speed motor.

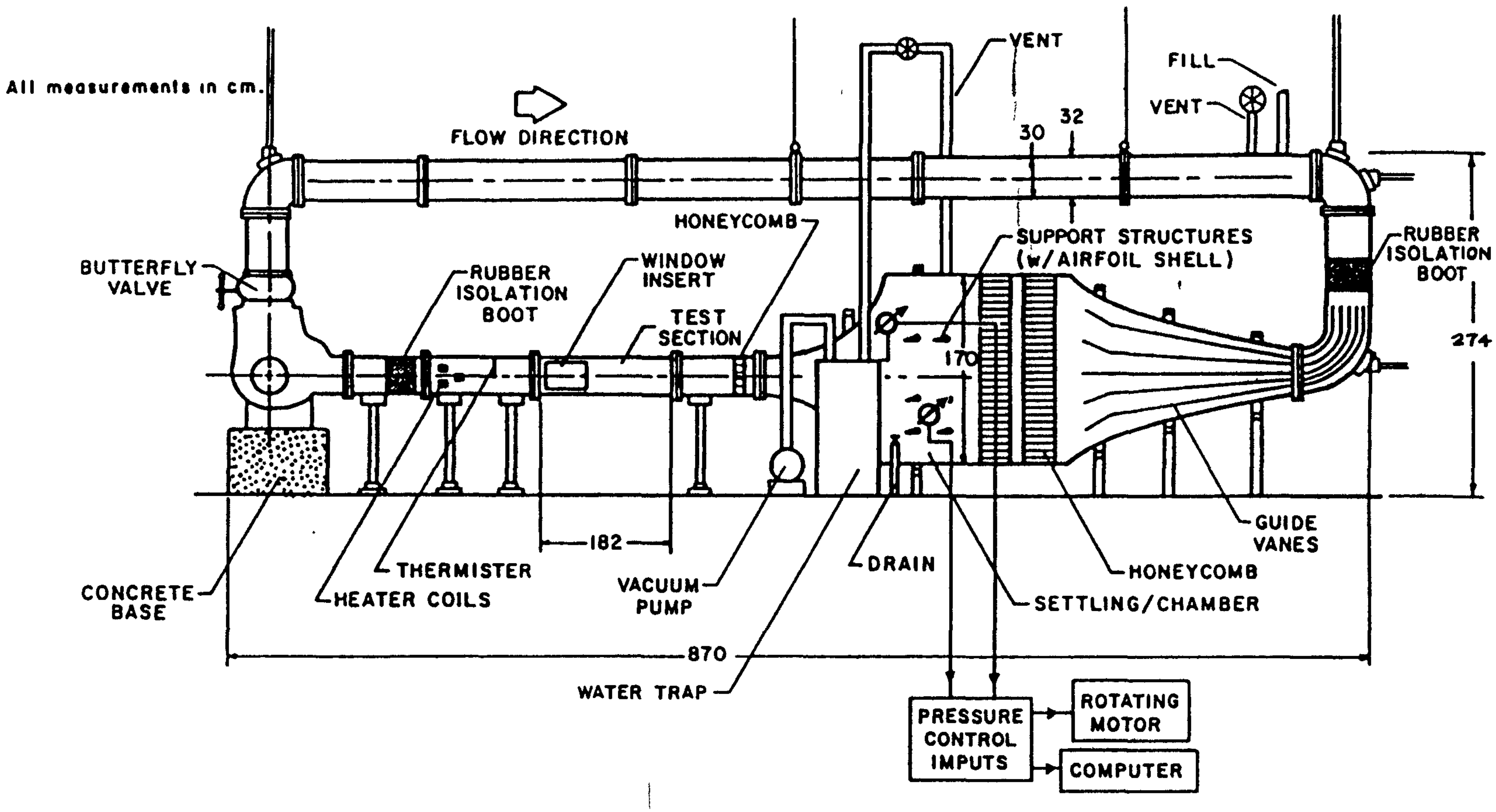

Fig. 2 The ESM water tunnel showing the water trap, the vacuum pump and controls recently installed.

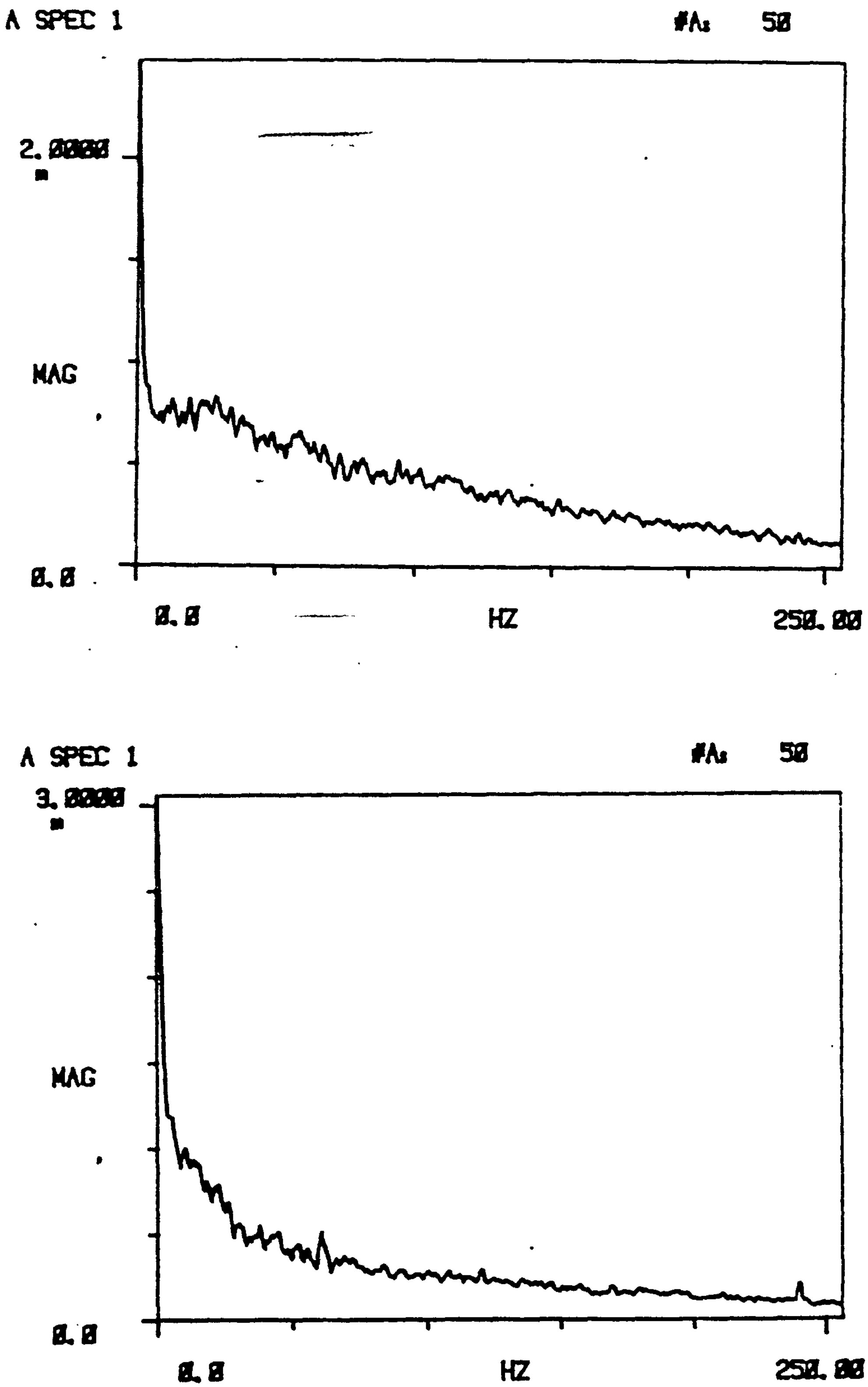

Fig. 3 Velocity spectra in the water tunnel obtained after the new honeycomb and screens were added in the settling chamber. The spectrum on top was obtained with an extra honeycomb at the entrance to the settling chamber.

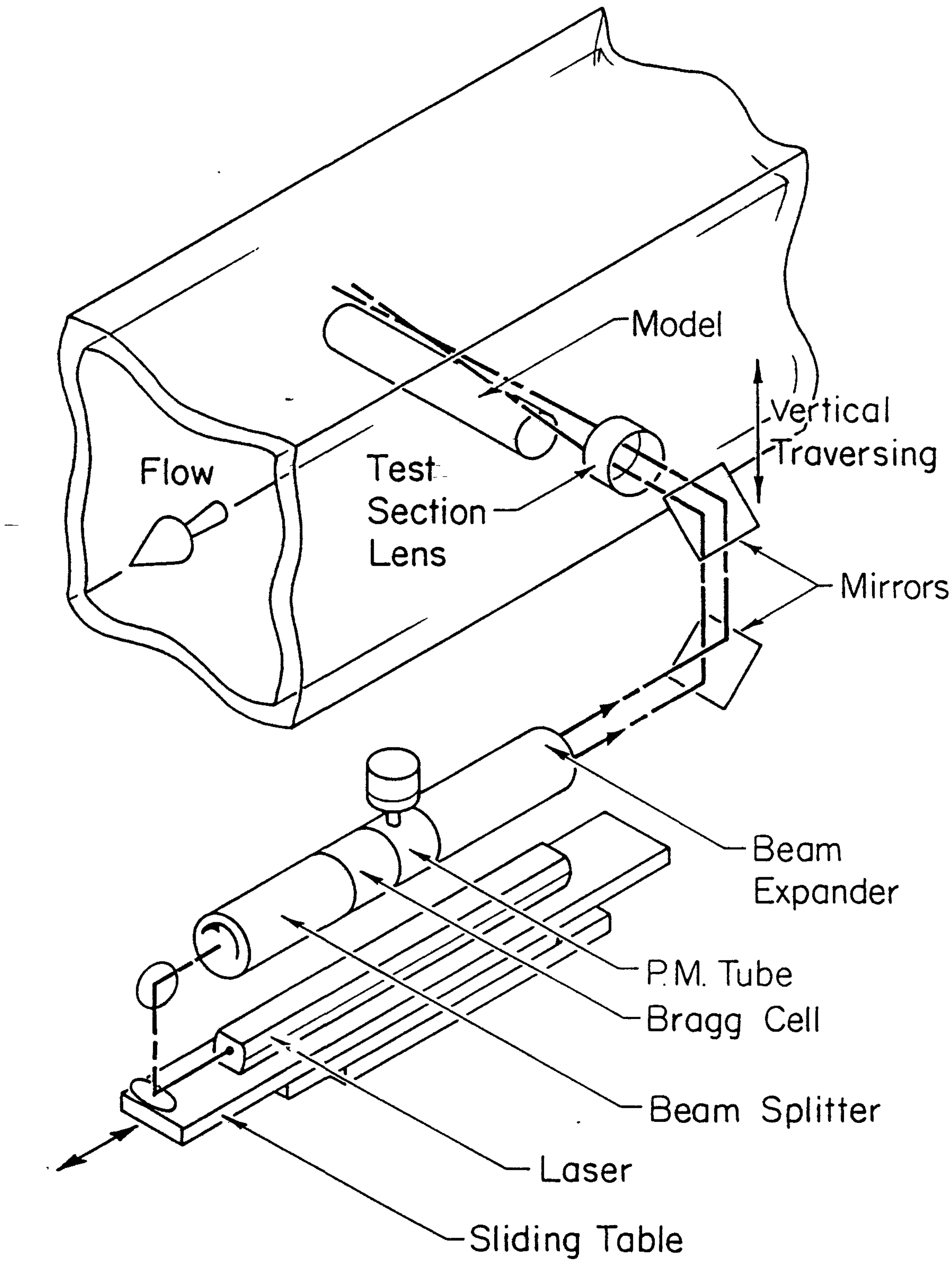

Fig. 4 Laser-Doppler arrangement mounted on a sliding table which is controlled by a stepping motor.

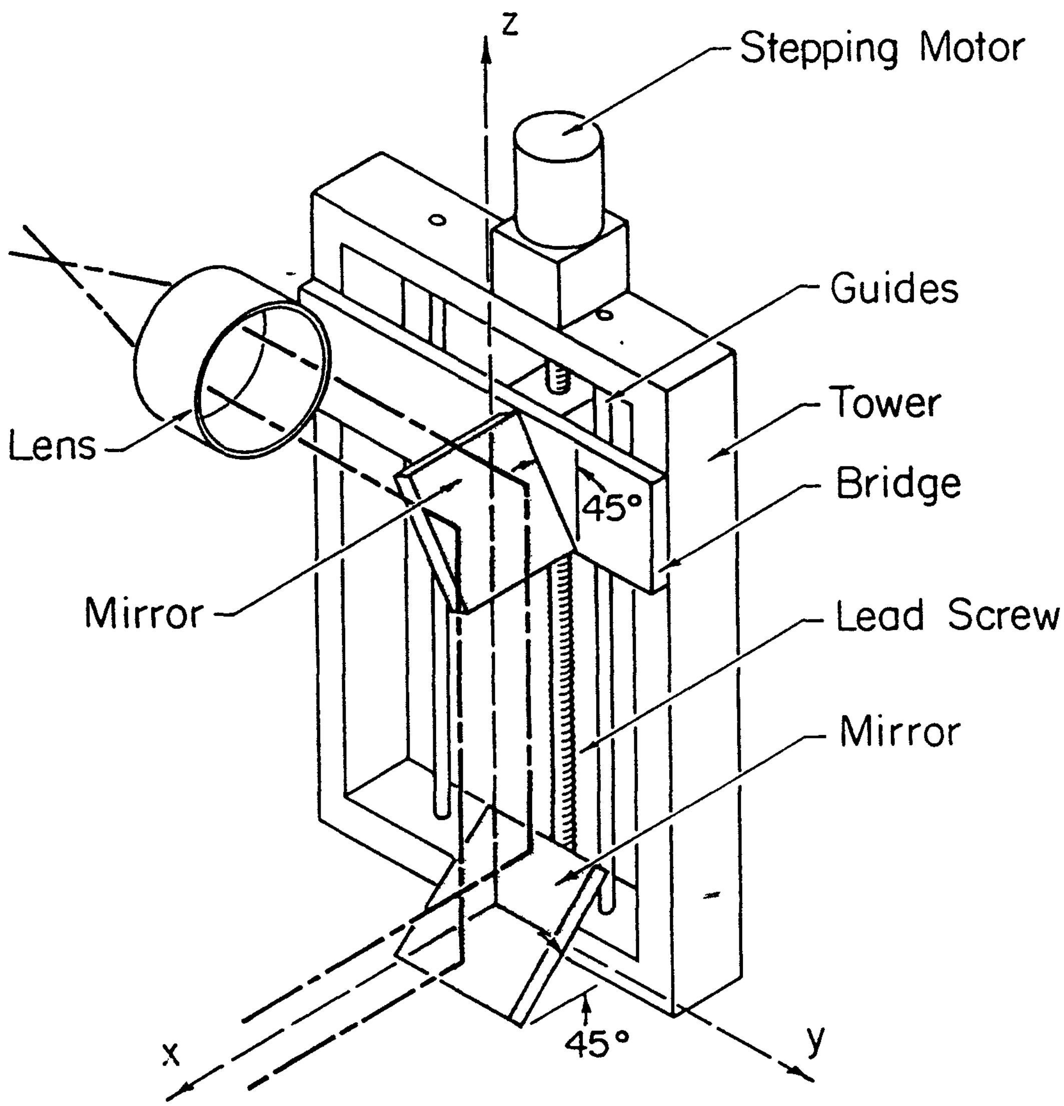

Fig. 5 The traversing mechanism designed and constructed to control the vertical motion of the measuring volume.

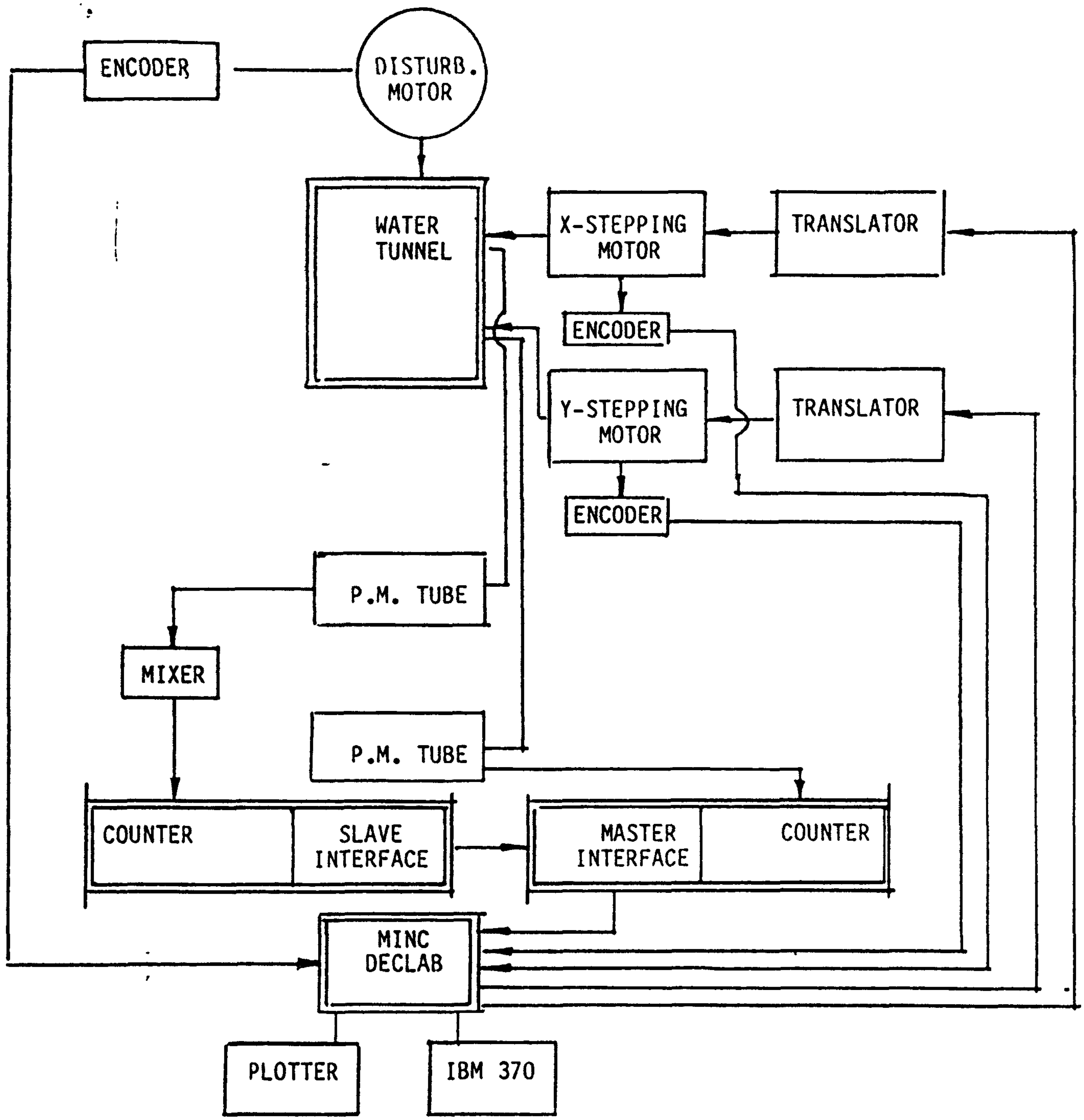

Fig. 6 Arrangement of the equipment for obtaining and reducing the data.

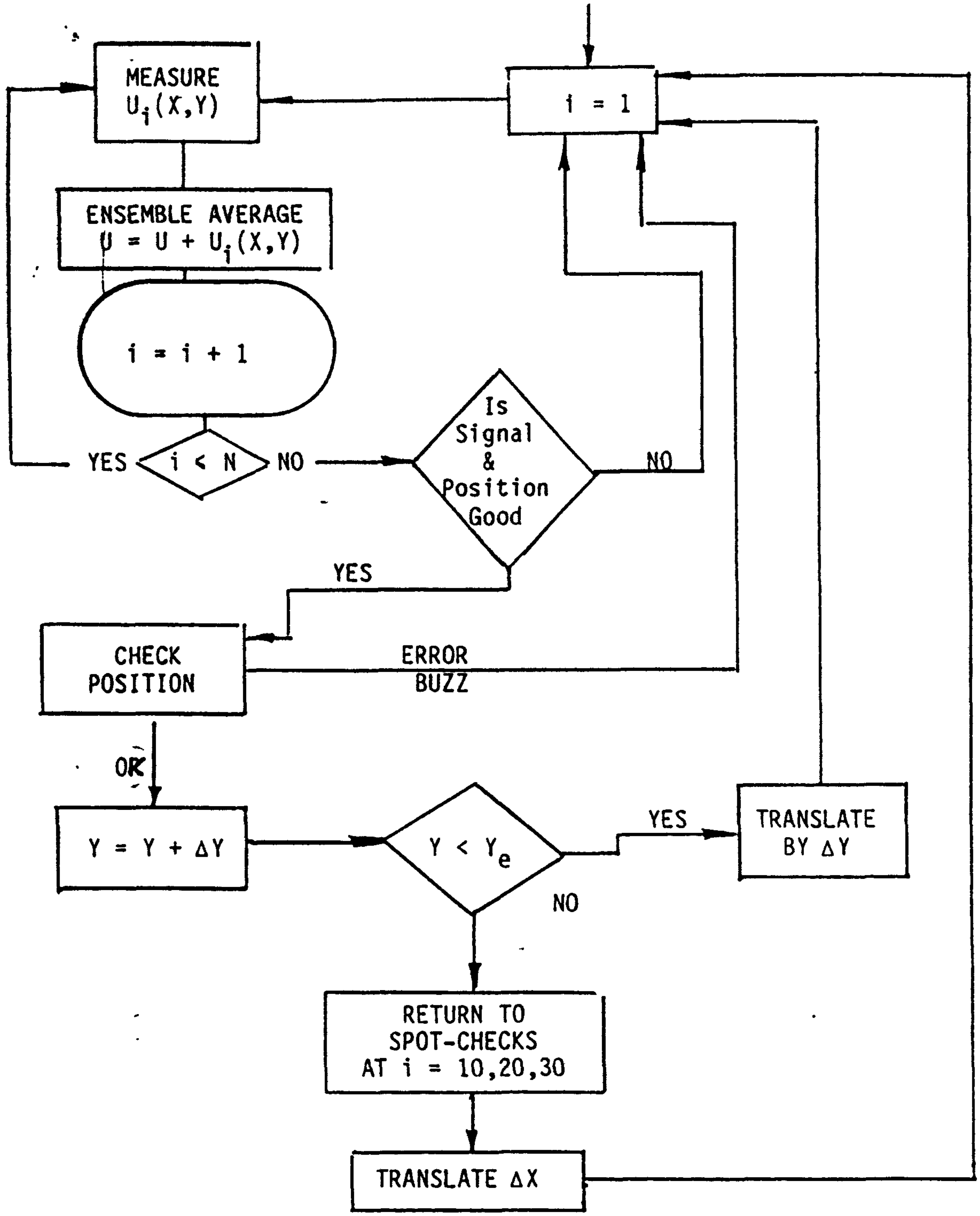

Fig. 7 Flowchart for data acquisition.

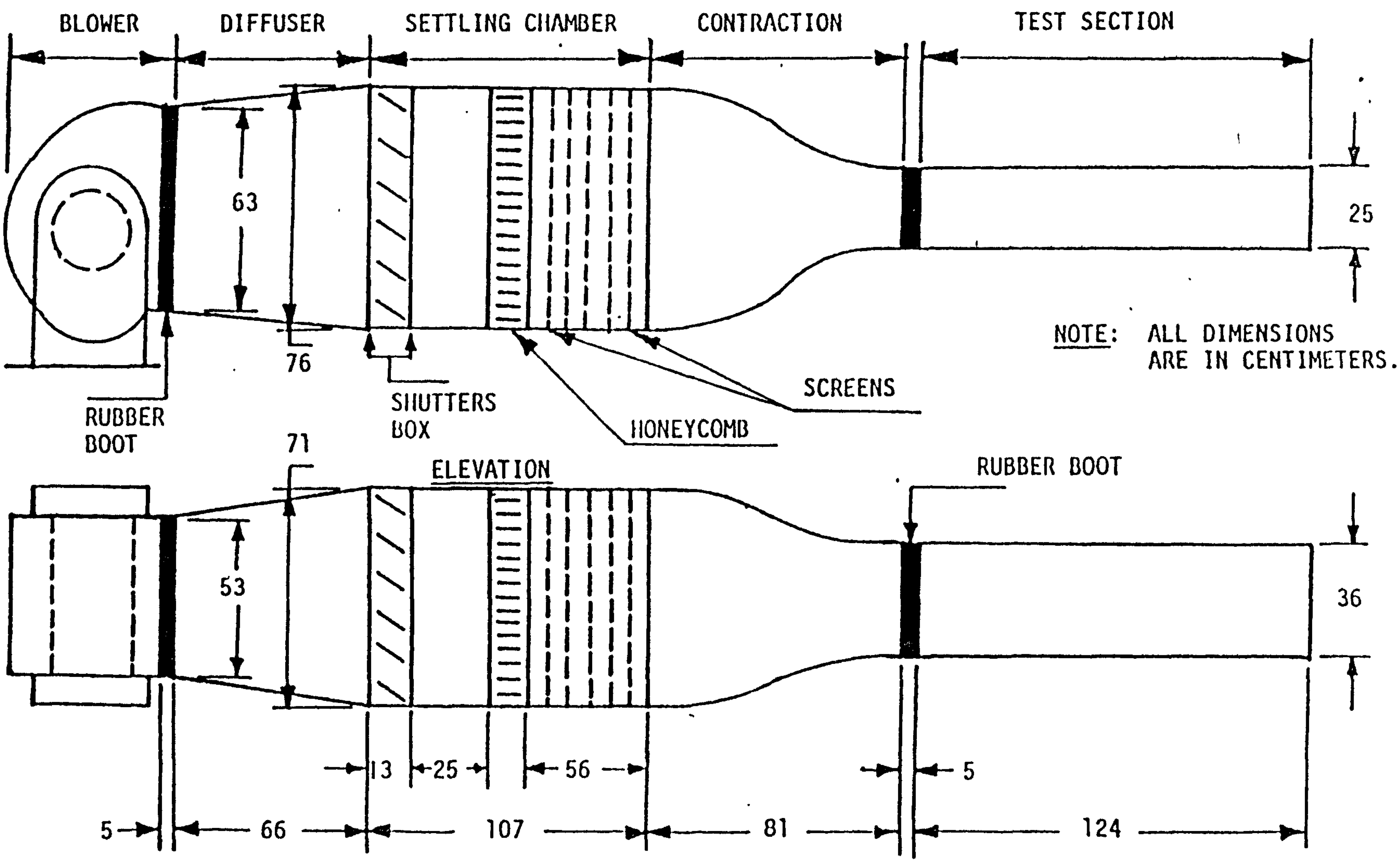

FIGURE 8: THE PULSATING FLOW WIND TUNNEL

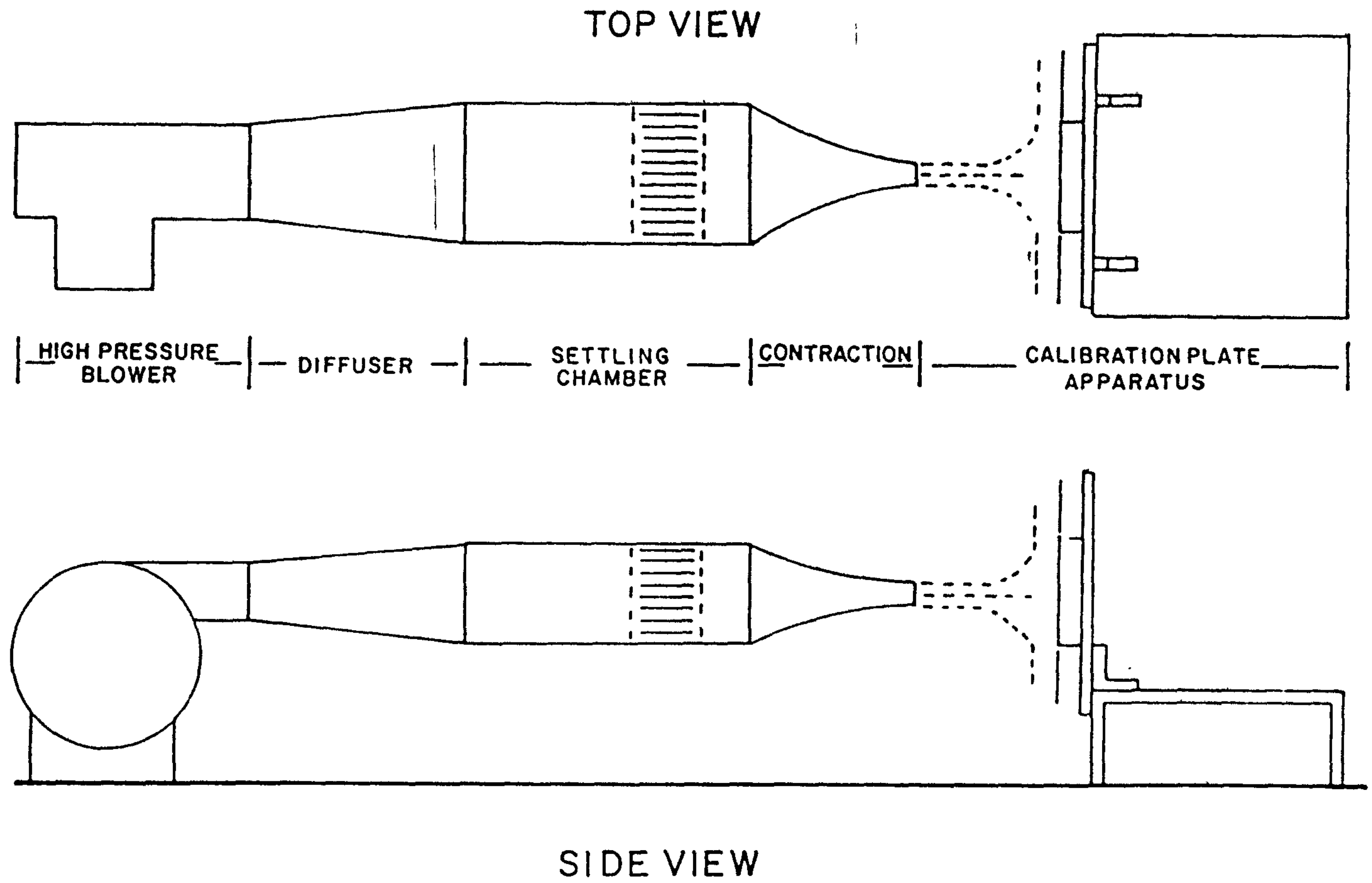

Fig. 9 The flow system.

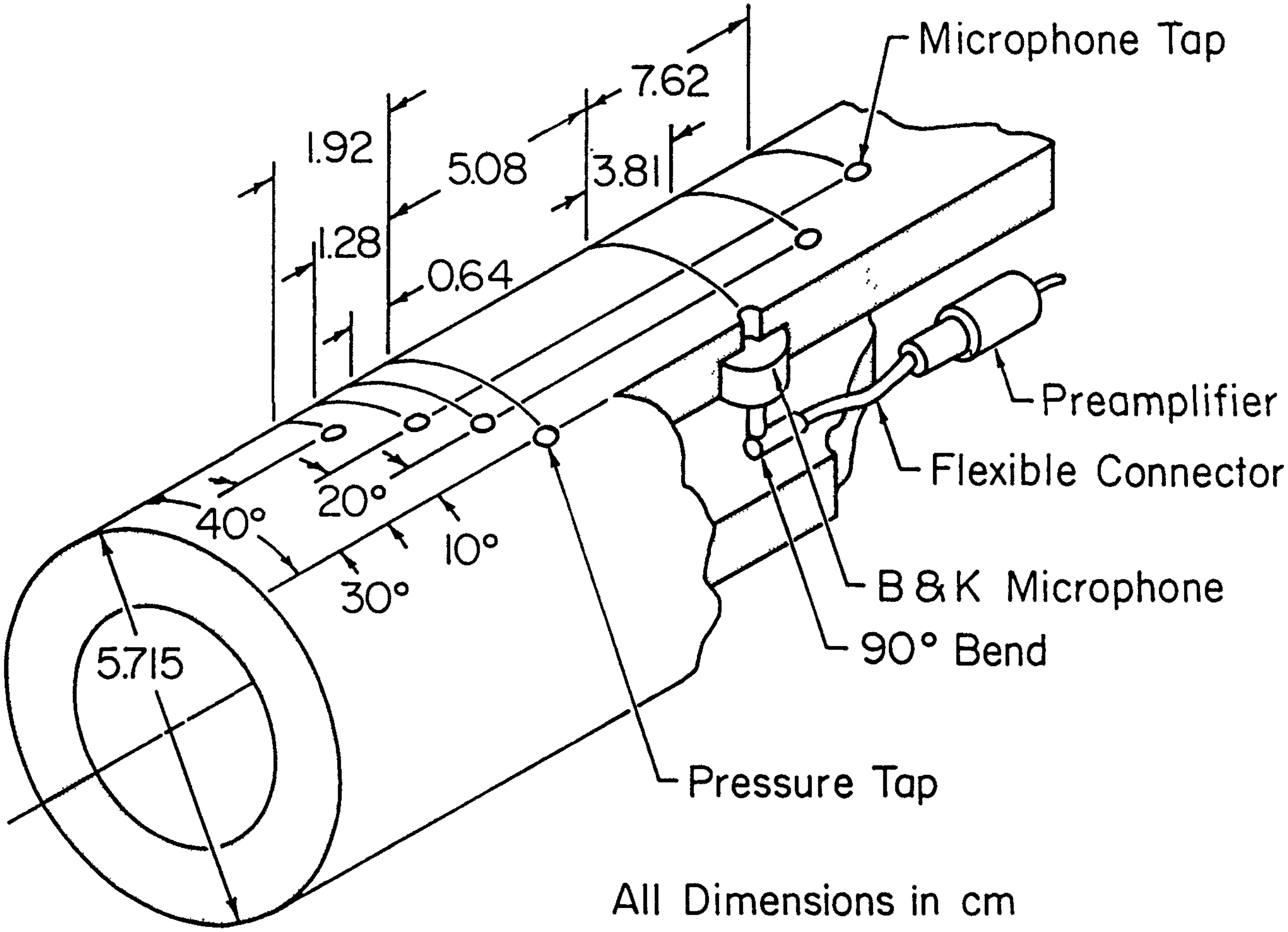

Fig. 10 The model for mean and instantaneous pressure measurement.

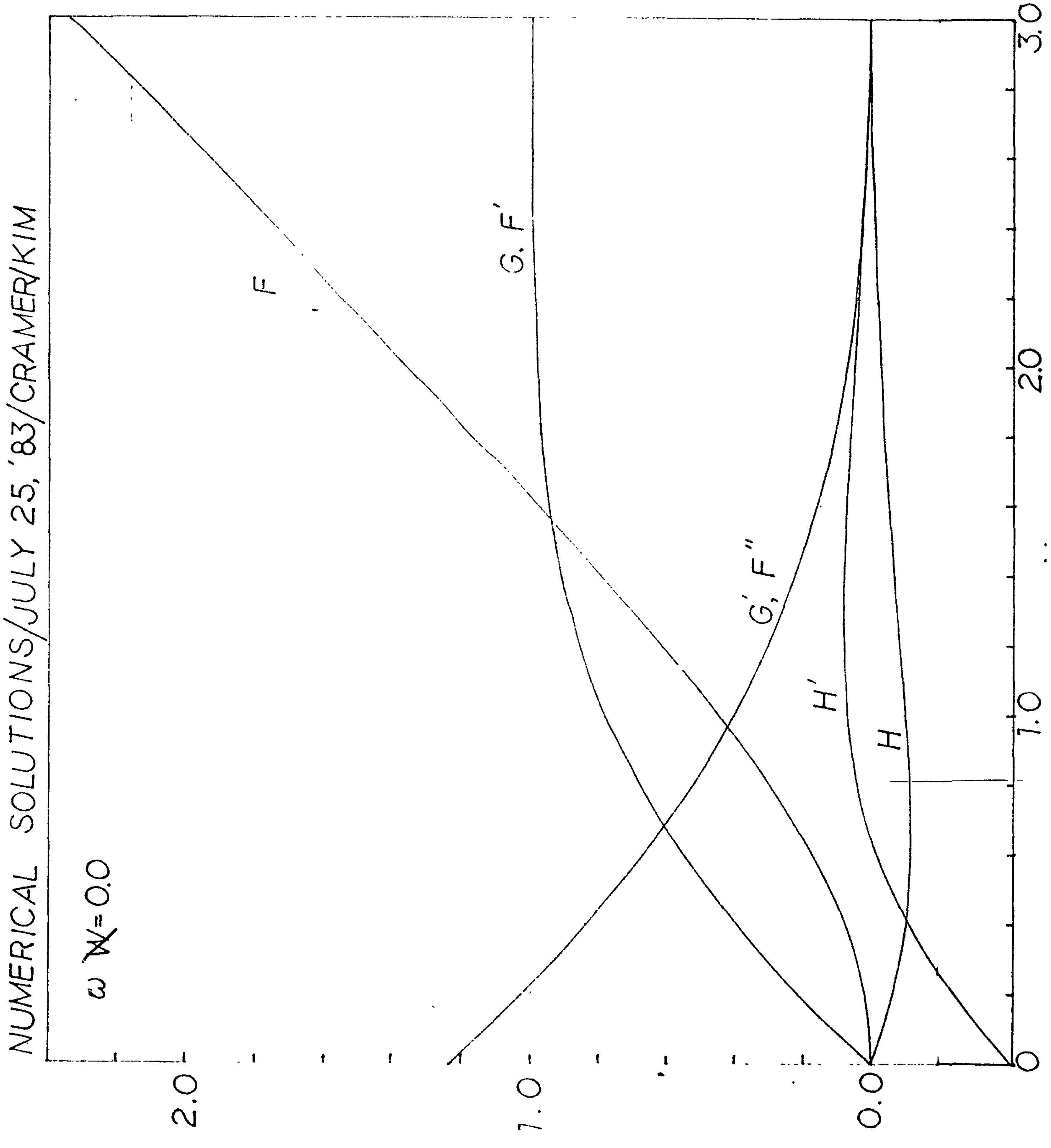

Fig. 11 The functions of the expansions of the stagnation flow solution.

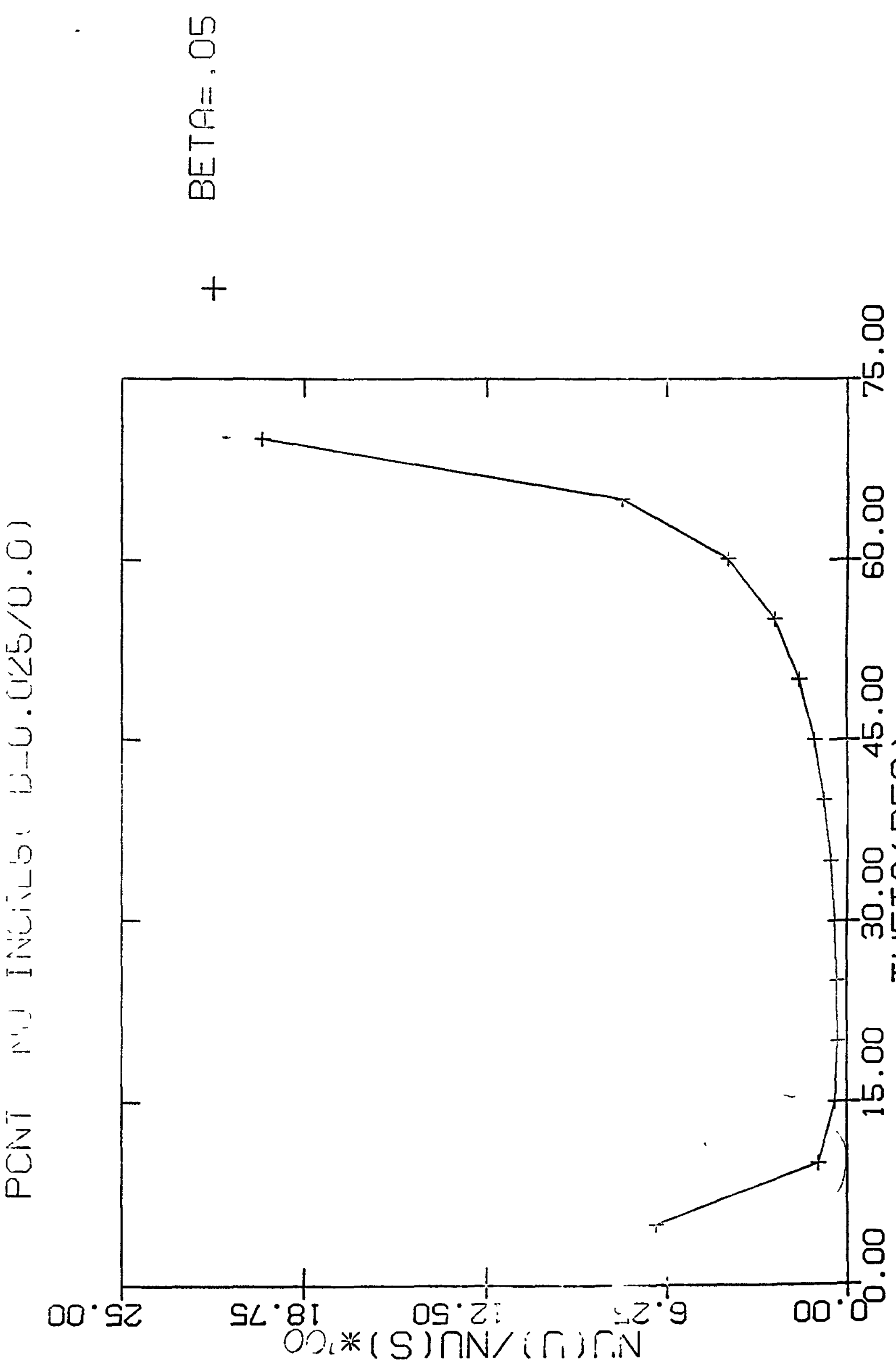

Fig. 12 The averaged heat transfer for an amplitude of oscillation of 5%.